On the genetic architecture of rapidly adapting and convergent life history traits in guppies

Author list:

James R Whiting[1], Josephine R Paris[1], Paul J Parsons[1,2], Sophie Matthews[1], Yuridia Reynoso[4], Kimberly A. Hughes[3], David Reznick[4], Bonnie A Fraser[1]

Author Affiliations:

1) Department of Biosciences, University of Exeter, Stocker Road, Exeter EX4 4QD, UK
2) Department of Animal and Plant Sciences, University of Sheffield, Alfred Denny Building, University of Sheffield, Western Bank, Sheffield S10 2TN, UK
3) Department of Biological Science, Florida State University, Tallahassee, Florida, 32303, USA
4) Department of Biology, University of California Riverside, Riverside, California, 92521, USA

Corresponding Author:

James R Whiting: jwhiting2315@gmail.com

Keywords:

Guppy, Quantitative Genetics, Life History Traits, Rapid Adaptation, Convergent Evolution, Parallel Evolution, QTL.

ABSTRACT

The genetic basis of traits can shape and constrain how adaptation proceeds in nature; rapid adaptation can be facilitated by polygenic traits, whereas polygenic traits may restrict re-use of the same genes in adaptation (genetic convergence). The rapidly evolving life histories of guppies in response to predation risk provide an opportunity to test this proposition. Guppies adapted to high- (HP) and low-predation (LP) environments in northern Trinidad evolve rapidly and convergently among natural populations. This system has been studied extensively at the phenotypic level, but little is known about the underlying genetic architecture. Here, we use an F2 QTL design to examine the genetic basis of seven (five female, two male) guppy life history phenotypes. We use RAD-sequencing data (16,539 SNPs) from 370 male and 267 female F2 individuals. We perform linkage mapping, estimates of genome-wide and per-chromosome heritability (multi-locus associations), and QTL mapping (single-locus associations). Our results are consistent with architectures of many-loci of small effect for male age and size at maturity and female interbrood period. Male trait associations are clustered on specific chromosomes, but female interbrood period exhibits a weak genome-wide signal suggesting a potentially highly polygenic component. Offspring weight and female size at maturity are also associated with a single significant QTL each. These results suggest rapid phenotypic evolution of guppies may be facilitated by polygenic trait architectures, but these may restrict gene-reuse across populations, in agreement with an absence of strong signatures of genetic convergence from recent population genomic analyses of wild HP-LP guppies.

INTRODUCTION

Recent evidence that phenotypes can evolve rapidly and often with surprising repeatability (convergence) has led to a re-evaluation of our expectations surrounding adaptation in nature. Particularly, understanding the genetic architecture of traits associated with both rapid adaptation and convergence can allow for insights into how adaptive variation may be maintained and be made available to respond to sudden changes in selection. Such research is important not only due to the current global circumstances of rapid environmental change, but also to understand adaptation more generally. Quantitative traits can have architectures made up of many loci of small effect (polygenic), single loci of large effect (monogenic), or an intermediate of these (oligogenic). There are currently theoretical expectations surrounding which of these are most likely to underlie rapidly adapting (Pritchard *et al.*, 2010; Jain and Stephan, 2017b) and/or convergent phenotypes (Yeaman *et al.*, 2018) but empirical evidence is only starting to accumulate.

Polygenic traits may facilitate rapid adaptation by providing a substrate of standing genetic variation to be exploited (Jain and Stephan, 2015, 2017a; Barghi *et al.*, 2019), enabling populations to adapt to shifting fitness optima by many small changes (Jain and Stephan, 2017b). Indeed, Fisher's fundamental theorem states that the rate change of mean fitness is equal to the amount of additive genetic variance for fitness (Fisher, 1930). Conversely, rapid adaptation of oligogenic traits is expected to occur through selective sweeps, which can result in less precise shifts across the fitness landscape or 'overshooting' incurring genetic load (Buffalo and Coop, 2019). On the basis of this cost, it is expected that most rapid adaptation of modest changes to trait means should occur using many loci of small effect, with the exception of instances in which sudden environmental change is so extreme as to

be lethal and affect absolute fitness (Bell, 2013; Whitehead *et al.*, 2017). Recent examples of suspected polygenic bases involved in rapid adaptation include shell morphologies of *Littorina* periwinkles (Westram *et al.*, 2018), immunity phenotypes in response to myxomatosis in rabbits (Alves *et al.*, 2019), and killifish adapting to anthropogenic thermal effluent runoff (Dayan *et al.*, 2019).

Similarly, there are expectations regarding the interactions between genetic architecture and convergent evolution. Whilst convergent phenotypes can arise through non-convergent genetic routes, the likelihood of convergent phenotypes having convergent genetics is expected to vary according to trait architecture. For example, polygenic traits reduce the likelihood of evolution of the same genes by increasing redundancy in the mapping of genotype to phenotype (Yeaman *et al.*, 2018; Barghi *et al.*, 2020; Láruson *et al.*, 2020). In contrast, if genetic architectures are simple and composed of few large effect loci, reduced redundancy can funnel adaptation through repeatable genetic paths. Many of the most notable examples of genetic convergence are single loci of large effect (Stern, 2013), including the *eda* gene associated with marine-freshwater armour plate phenotypes in three-spined stickleback (Colosimo, 2005), and the *optix* gene associated with wing patterning across *Heliconius* species (Reed *et al.*, 2011).

The guppies of northern Trinidad are a model system for studying phenotypic adaptation, which has provided empirical evidence for both rapid adaptation and convergent evolution. In this system, barrier waterfalls within many rivers have created replicated downstream/high-predation (HP) and upstream/low-predation (LP) habitats. Each river contains HP- and LP-adapted guppy populations that have independently evolved

71 convergent LP phenotypes in predator-free upstream environments. LP populations are
72 typically longer-lived, exhibiting larger adult sizes, reduced brood size, longer time to reach
73 maturity and longer interbrood period than their HP counterparts (Reznick, 1982; Reznick *et*
74 *al.*, 2001; Torres Dowdall *et al.*, 2012). Experimental translocations of HP guppies to
75 previously uncolonised LP environments further demonstrated that LP life history
76 phenotypes evolve rapidly (Endler, 1980; Reznick and Bryga, 1987; Reznick *et al.*, 1990,
77 1997, 2019; Gordon *et al.*, 2009). Guppies raised under laboratory conditions for multiple
78 generations continue to exhibit differences between HP and LP phenotypes, indicating these
79 traits have a heritable genetic basis (Reznick, 1982; Torres Dowdall *et al.*, 2012). Beyond this
80 however, and despite the wealth of knowledge regarding life history evolution in these
81 populations, little is known about the genetic architecture of these traits.
82
83 Life history traits are typically quantitative and are commonly involved in adaptation to
84 novel or changing environments. Previous studies exploring the genetic basis of life history
85 traits have documented everything from highly polygenic traits, such as clutch size and egg
86 mass in great tits (Santure *et al.*, 2013) and weight of Soay sheep (Bérénos *et al.*, 2015), to
87 traits with single loci explaining a large proportion of phenotypic variance, such as age at
88 maturity in atlantic salmon (*Salmo salar* L) (Ayllon *et al.*, 2015; Barson *et al.*, 2015) and other
89 salmonids (Moghadam *et al.*, 2007; Kodama *et al.*, 2018). Life history traits can often exhibit
90 genetic covariance, with different traits sharing aspects of their genetic architecture, which
91 can have important implications for pleiotropic constraint during adaptation (Hall *et al.*,
92 2006).
93

There are various avenues for exploring the genetic architecture of quantitative traits. For example, single locus quantitative trait locus (QTL) analyses or Genome-Wide Association Studies (GWAS) are now commonplace. However, these approaches can inflate the prominence of single loci and their inherent bias against multi-locus models has come under scrutiny (Rockman, 2012; Slate, 2013). Indeed, multi-locus analyses have resolved some empirical inconsistencies, such as the "missing heritability crisis" (Manolio *et al.*, 2009), subsequently returning much higher estimates of heritability compared with the sum of single-locus outliers for classic quantitative traits such as human height (Yang *et al.*, 2010; Yang, Manolio, *et al.*, 2011). Extensions of these multi-locus approaches have partitioned phenotypic variance into specific chromosomes, with correlations between chromosome size (as a proxy for number of functional loci) and partitioned phenotypic variance taken as evidence for highly polygenic traits (Santure *et al.*, 2013; Bérénos *et al.*, 2015; Kemppainen and Husby, 2018a). The rising prominence of multi-locus models has started to bring empirical evidence back in line with Fisher's prediction of the importance of many loci of small effect, often dubbed the "infinitesimal model" (Fisher, 1918; Barton *et al.*, 2017). It is therefore important to explore analyses that allow for all possible trait architectures.

Using an F2 breeding cross design, we examine the genetic basis of seven life history traits in guppies: female age (1) and size (2) at first brood, first brood size (3), interbrood period (4), average dry offspring weight in the first brood (5), and male age (6) and size (7) at maturity. Our aims are to assess the relative extents to which different facets of life history traits have significant genetic elements, and whether guppy life history traits are better explained by polygenic, oligogenic, or monogenic models. By exploring the genetic bases of these traits within a system for which rapid adaptation and convergent evolution is already

well-documented, we can better understand the role of quantitative genetic architecture in these processes.

METHODS

Crosses

Fish were second and third generation lab-reared individuals from an HP site in the Yarra river (680415E, 1193791N) and an LP site in the Quare river (696907E, 1181003N) (Figure 1). These populations have demonstrable HP-LP life history phenotypes (Table S1), and have been studied extensively in prior work (Reznick, 1982; Reznick *et al.*, 1996, 2004, 2005). Four F2 full-sib intercrosses were performed. Two crosses were performed for each cross direction in which wild-caught LP males were crossed with wild-caught HP females and vice versa. F1s were mated within cross and F2s were phenotyped and genotyped. Grandparents were also genotyped.

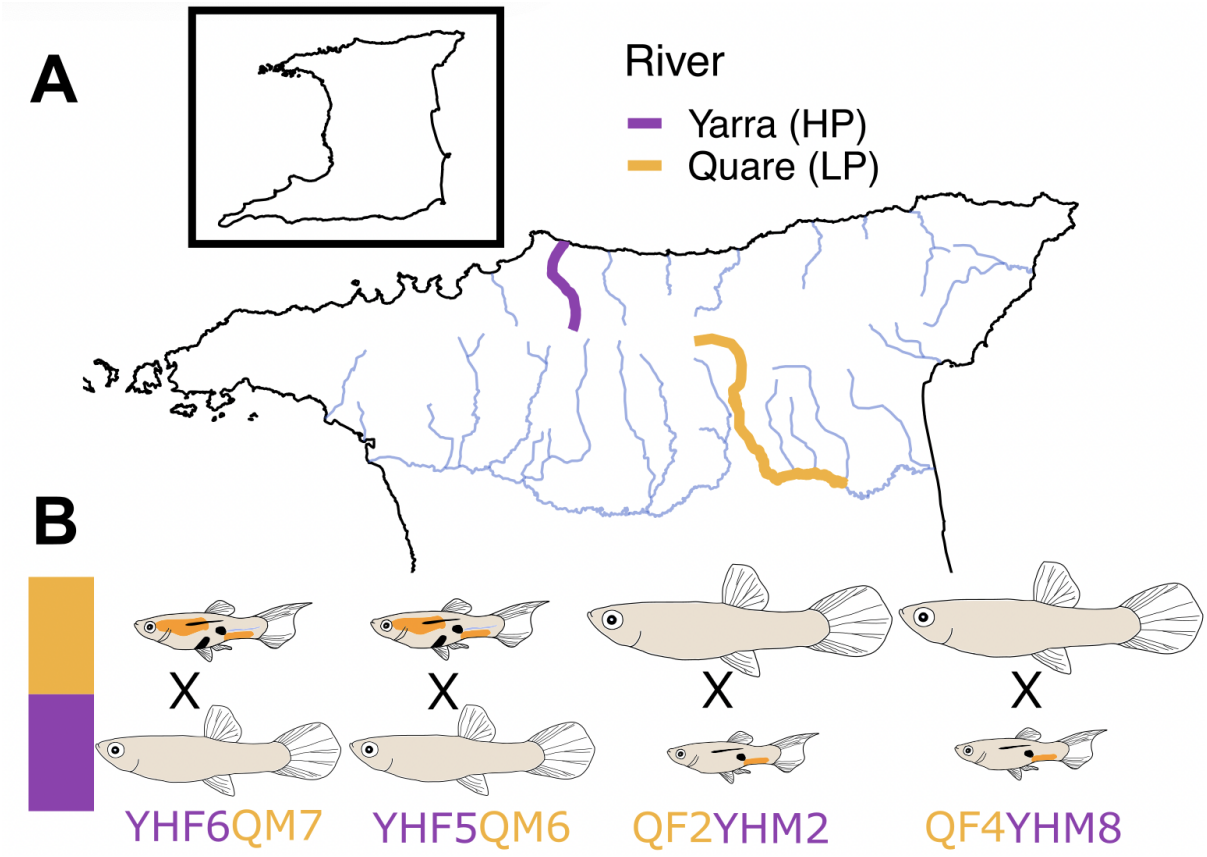

Figure 1: Sampling rivers in Trinidad and cross design. Sampling rivers are highlighted along with a number of major rivers from northern Trinidad's three drainages (**A**). Four families were produced from eight grandparents (**B**), two for each cross direction. Males (smaller, colourful) and females (larger, uncoloured) in panel **B** also highlight common morphological differences between HP (smaller, less colourful) and LP individuals.

Phenotyping and Phenotype GLMs

Life history phenotyping and rearing followed (Reznick, 1982); full rearing details are available in the supplementary materials. Size of females and males was measured under a dissecting scope with Vernier calipers following MS-222 anaesthetisation. Based on the allometric dependency of female brood size, we took residual brood size as the residual difference between observed and linear-predicted brood size based on size. Male age at maturity was judged from the development of the apical hook. Interbrood period was scored as days between first and second parturition. Offspring weight was recorded as the

mean dry weight of individuals from the first litter (data from the second litter was highly correlated). Where necessary, phenotypes were log-transformed to improve fit for normality assumptions.

Rearing (mean temperature and date of birth (DOB)) and family effects on phenotypes were explored using generalized linear models (GLM) in R (v4 (R Core Team, 2020)). DOB was included as a proxy for subtle unmeasured changes in rearing conditions over time. We used backwards model selection implemented in *step()*, starting from an additive model including family, temperature, and DOB. Relevant model assumptions were checked by comparing residuals to simulated residuals in the R package *DHARMa* (Hartig, 2020). Final model term significance was determined by comparing models with and without each independent variable using *drop1()* in terms of ΔAIC and using F-tests. Where model assumptions could not be met, final model terms were taken and significance ($p < 0.05$) of Spearman's rank correlations were used to confirm model effects. Adjusted partial R-squared was estimated for all final model variables with the R package *rsq (Zhang, 2020)* using the variance-function-based type.

Genotyping

Genomic DNA was extracted from fin clips using an ammonium acetate extraction method (Nicholls *et al.*, 2000; Richardson *et al.*, 2001). We genotyped each individual using a RAD-seq library preparation method adapted from Poland and colleagues (Miller *et al.*, 2007; Baird *et al.*, 2008; Poland *et al.*, 2012); full genotyping details are available in the supplementary materials. Of all 661 individuals used in the final analysis, 61 were sequenced two or three times in separate libraries to account for low coverage ("merged"

172 individuals in Table S2). To ensure optimal coverage, and reduce PCR duplicate effects, all
173 eight grandparents were sequenced four times in four separate PCR reactions and
174 sequencing libraries. Of the total 653 F2s, 637 (370 males, 267 females) were used for
175 phenotype analyses due to missing phenotypes for 16 individuals.
176
177 ***Bioinformatic processing***
178 Raw read data were trimmed and adaptors removed using cutadapt (Martin, 2011). Stacks
179 v2.5 was used for all downstream processing (Rochette *et al.*, 2019). Trimmed read data
180 were used as input in process_radtags, with options to remove reads with uncalled bases (-
181 c), quality filter at Q10 (-q), and rescue barcodes and RAD tags containing sequencing error
182 (-r). Cleaned RAD tags were aligned to the male guppy reference genome using BWA-MEM
183 (Li, 2013), and converted to bam format using samtools. Read group information was added
184 to bam files using Picard Tools v2.6.0 AddOrReplaceReadGroups (Broad Institute, 2019) and
185 alignments based on the same individual were merged using Picard Tools MergeSamFiles.
186 Bam files were used as input for the gstacks module in Stacks2, using only alignments with a
187 minimum mapping quality of 20. The final VCF contained only loci called across all
188 individuals (-p 1), at a max-missing frequency of 80% (-r 80) and minor allele frequency (-
189 maf) of 5%. Samples were retained with ≥ 15X average coverage, average coverage across
190 the samples was 33.4X (Table S2) and average missing data was 0.05%. For QTL scans
191 genotypes were imputed based on grandparental phasing (see below).
192
193 ***Linkage mapping***
194 Linkage maps were produced with Lep-MAP3 (Rastas, 2017). Pedigrees were produced for
195 each cross by including dummy parents (one pair per cross) from which all F2s descended.

Genotype likelihoods were called from the VCF input with the *ParentCall2* module, including the *-halfSibs=1* flag. Further filtering was performed with the *Filtering2* module removing markers with a MAF < 0.1 (within families) and with missing data in >10% of individuals (within families). Markers were mapped to linkage groups (LG) with *SeperateChromosomes2* modules based on a logarithm of the odds (LOD) score of 20, using all informative markers, and grandparental phase information. LGs with fewer than 20 markers were discarded, leaving 21 LGs. The two largest LGs were separated by further iterations of *SeparateChromosomes2* run over these specific LGs with an elevated LOD limit of 30. This produced 23 LGs in agreement with the guppy genome. Unmapped markers were joined to the 23 LGs with the *JoinSingles2All* module, with an LOD limit of 5. The module was iterated until no further markers could be mapped. In total, 7,256 markers of 16,539 were mapped to LGs. The module *OrderMarkers2* was then run over each LG independently to order and place markers within LGs. An initial 10 iterations were performed, with order determined by maximum likelihood. For chromosome 12, male recombination was not permitted given previous evidence that males do not recombine over the sex chromosome (Charlesworth, Zhang, *et al.*, 2020). LOD scores from these maps were used to further filter markers on the basis of support for multiple mapping within a LG (multiple LOD peaks) or if maximum LOD was within one standard deviation of the mean. These markers were blacklisted for the final *OrderMarkers2* run, in which the *evaluateOrder* flag was run over the earlier maximum-likelihood based map. Final maps were sex-averaged and trimmed according to graphical evaluation. Grandparental-phased genotypes were exported for QTL analysis. Effects of female-biased heterochiasmy (Bergero *et al.*, 2019) on linkage maps are discussed in the supplementary material.

220 ***Heritability and multi-locus estimates of trait architecture***

221 We used Genome-wide Complex Trait Analysis (GCTA) (Yang, Lee, *et al.*, 2011) to estimate
222 phenotype heritability. This approach estimates the heritability of phenotypes by
223 partitioning phenotypic variance into genetic variance (specifically of the SNPs sequenced
224 rather than heritability in the traditional sense), random genetic effects and residual
225 variance using the restricted maximum likelihood (REML) method within a linear mixed
226 model. Empirical support suggests that heritability estimates using this method are
227 comparable to those estimated from true pedigree studies (Stanton-Geddes *et al.*, 2013;
228 Duntsch *et al.*, 2020). We first separated SNP data into males and females and, for each,
229 estimated a genetic relatedness matrix (GRM) using all SNPs. SNPs from scaffolds were
230 merged onto the beginning/end of chromosomes according to the linkage map (Table S3) to
231 improve the accuracy of per-chromosome estimates. To account for genetic variance among
232 the four families, we included the first three eigenvectors from PCA (the minimum number
233 required to separate four families) as quantitative covariates. Specifically, these analyses are
234 assessing within-family associations between genetic covariance and phenotypic variance,
235 and allowing for among-family intercepts to vary. Rearing covariates were included in a
236 trait-specific manner if these were associated with the phenotype (Table S4). To assess
237 within-family effects, we included an additional GRM calculated with the *--make-bK 0.05*
238 parameter. The addition of this GRM allows us to partition variance into that associated
239 with sequenced SNPs (G1) and within-family structure (G2). At the per-chromosome level,
240 including this additional GRM prevented model convergence in some cases (11/138
241 chromosome-phenotype pairs), but we observed negligible differences in heritability
242 estimated with and without this additional GRM at the whole-genome level.
243

To estimate the heritability associated with specific chromosomes (h^2c), we took two approaches: 1) We partitioned phenotypic variance using a model with a GRM derived from the focal chromosome and quantitative covariates; 2) We used a likelihood-ratio test (LRT) approach following (Santure *et al.*, 2013, 2015; Duntsch *et al.*, 2020) in which we compared a full model *a* (GRM based on all chromosomes except focal chromosome + focal chromosome GRM) to a reduced model *b* (without focal chromosome GRM). Quantitative covariates were included in both models. Models were compared with a LRT according to (1), with p-values taken from the chi-squared distribution with one degree of freedom.

$$LRT = -2(L_a - L_b) \qquad (1)$$

Correlations can reveal polygenic architectures. Positive correlations suggest traits are associated with many loci of small effect, assuming chromosome size is a proxy for functional loci count. Previous work has suggested p-values derived from both chromosome partitioning approaches highlighted above are comparable (Kemppainen and Husby, 2018a), so we used h^2c estimations from focal chromosome GRMs (approach 1) as issues with model convergence prevented estimations of h^2c on chromosomes that accounted for little phenotypic variance under approach 2 (see Table S5). Regressions were performed using the *HC_Correction()* function presented by Kemppainen and Husby (2018b), which corrects for heteroscedasticity among chromosomes and the constraint of GCTA models that prevents negative estimations of h^2c.

QTL scans

We produced two datasets for QTL-scanning. The first included fully-informative SNPs for both founding populations, i.e. SNPs that were homozygous in all eight grandparents and fixed for alternative variants between HP and LP-derived grandparents. This dataset included 1,220 SNPs, and allowed for analysis of all individuals together to increase biological power, where individuals could inherit an HP (H) or LP (L) allele. The second dataset comprised four separate datasets, one for each family in which family-informative SNPs were included for each family (homozygous, alternative, SNPs in each grandparent within families). Numbers of family-informative SNPs for each family were similar (3,436; 3,400; 3,476; and 3,476 for QF2YHM2, QF4YHM8, YHF5QM6, and YHF6QM7 respectively). These datasets provided weaker biological power, but increased resolution within families, and also allowed us to examine alleles that may have only been captured and are segregating in single crosses. It is important to note, these latter datasets cannot be used to assess loci that are Y-linked. Because all males within a family carry the same Y, the effect of different Y loci among families cannot be separated from general genome-wide relatedness within and among families that captures many autosomal loci.

We first performed single locus scans using the *scan1()* function in R/qtl2 (Broman *et al.*, 2019). We inserted pseudomarkers using *insert_pseudomarkers()* with step=1, calculated genotype probabilities with *calc_genoprob()* and an error_prob=0.002, and converted genotype probabilities to allele probabilities using *genoprob_to_alleleprob()*. We calculated a grid with *calc_grid()*, subsetted genotype probabilities to grid pseudomarkers with *probs_to_grid()*, and used this to calculate a kinship matrix with *calc_kinship()* according to the Leave-One-Chromosome-Out method (LOCO). Rearing covariates and a binary family assignment matrix were included as additive covariates . Significance of LOD peaks was

291 determined by 1000 permutations for all models with *operm()* at an α of 0.05. For scans of
292 the sex-determining region, inputs were merged for males and females, and the same
293 methodology was used, with the exceptions that sex was modelled as a binary phenotype,
294 and rearing covariates were excluded from the covariate matrix.
295
296 We also explored QTL scans that allow for multiple QTLs using the *stepwiseqtl()* function in
297 R/qtl (Broman *et al.*, 2003) which is not available in R/qtl2. This approach assesses
298 interactions among all pairs of loci, allowing for epistatic effects to be examined. We
299 allowed for models with a maximum of six loci, used the imputation method, and allowed
300 for only additive interactions among loci. Significance of LOD peaks was determined based
301 on 1000 permutations.
302

303 ## RESULTS

304 ### *Phenotypes*

305 Both male age (GLM: $F_{3,340} = 14.75$, $p = 4.82e^{-9}$) and size at maturity (GLM: $F_{3,340} = 16.02$, $p =$
306 $9.30e^{-10}$) of F2s varied significantly between the four cross families (Figure S1A; Table S4).
307 For age at maturity, cross YHF5QM6 F2s tended to mature later than all other crosses
308 (Tukey $p < 0.05$), and for size at maturity, cross QF4YHM8 F2s matured at a larger size. Male
309 age and size at maturity were not strongly associated with one another (correlation of
310 individuals, Spearman's ρ = -0.07, $p = 0.184$), but a GLM of male size at maturity by an
311 interaction between age at maturity and family revealed a significant effect (GLM: $F_{3,340} =$
312 2.98, $p = 0.031$). However, within this model relationships between male age and size at
313 maturity were both positive and negative depending on family. Rearing conditions affected
314 both male phenotypes. Males matured earlier under increased temperatures (GLM: $F_{1,340} =$

13.75, $p = 2.40e^{-4}$) and if born later in the experiment (GLM: $F_{1,340} = 23.26$, $p = 2.15e^{-6}$). Larger males at maturity tended to be born later in the experiment (GLM: $F_{1,340} = 41.51$, $p = 4.06e^{-10}$), but temperature did not affect size at maturity. Family status explained 10.4% and 11.7% of phenotypic variance for age and size at maturity respectively, which will not be captured by our subsequent mapping approaches.

Female phenotypes were generally less variable among families, only female size at first brood (GLM: $F_{1,265} = 11.88$, $p = 6.04e^{-4}$) and offspring weight (GLM: $F_{1,249} = 3.03$, $p = 0.030$) differed significantly between families (Figure S1B; Table S4), with the latter effect only marginally significant. Consistent with a general life history axis, covariance among female phenotypes was generally high (Table S6). All female traits loaded positively onto PC1 (37.6%), with female age (loading = 0.68) and size (loading = 0.58) loading particularly strongly. PC2 (27.0%) explained residual variance associated with brood traits, with first brood size (-0.62) and interbrood (-0.59) loading negatively, and offspring weight loading positively (0.44). PC2 therefore summarises variation among females with few, heavier offspring and short interbrood periods, and vice versa. Similar to males, females reached maturity and produced their first brood earlier under increased temperatures (GLM: $F_{1,265} = 21.65$, $p = 5.19e^{-5}$). Increased temperature also reduced interbrood period (GLM: $F_{1,265} = 24.32$, $p = 1.45e^{-6}$) and females born later in the experiment had longer interbrood periods (GLM: $F_{1,265} = 13.47$, $p = 2.94e^{-4}$). Other female phenotypes were not associated with rearing conditions (Table S4). In contrast to male phenotypes, family status explained much less phenotypic variance: 6.7% for first brood size, 5% for size at first brood, and 2.2% for offspring weight ('family' was dropped from other models due to low explanatory power).

339 ***Linkage mapping***

340 The final linkage map consisted of 6,765 markers and a length of 1,673.8 cM. There was
341 overall good concordance between this genetic map and the recently updated reference
342 genome (Fraser *et al.*, 2020), with the additional placement of unplaced scaffolds on all
343 linkage groups. There were also minor structural rearrangements and inversions (Figure S2),
344 for which corroborative support could be found from previously published HiC data (Fraser
345 *et al.*, 2020). Typically, unplaced scaffolds were joined to either chromosome end (Table S3;
346 Figure S2).

347

348 ***Heritability and multi-locus estimates of trait architecture***

349 Heritability varied between traits, but in almost all cases (excluding first brood size) the
350 variance explained by within-family structure (V_{G2}) was greater than the variance explained
351 by the specific SNPs themselves (V_{G1}). This is expected given RAD-sequencing is designed to
352 capture SNPs in linkage with causal variants, rather than causal variants themselves.
353 Estimates of heritability were greatest for male size at maturity (43.4%), offspring weight
354 (33.4%), male age at maturity (31.3%), and interbrood period (30.2%). Estimates for the
355 remaining female life history traits were lower, not exceeding 9.7% (female size at first
356 brood), with standard errors that overlapped 0 (Table 1).

357

358

359

360

361

Table 1: Estimates of genome-wide heritability for each phenotype based on GCTA-GREML. Phenotypic variance (V_P) is partitioned into variance explained by sequenced SNPs (V_{G1}), genetic family structure (V_{G2}) and residual variance (V_E). Final estimates of phenotypic variance partitions are given as proportions. All estimates include standard error.

Phenotype	V_{G1}	V_{G2}	V_E	V_P	V_{G1}/V_P	V_{G1+G2}/V_P
Age at first brood (F)	0 ± 0	0 ± 0	0.02 ± 0	0.02 ± 0	0.03 ± 0.19	0.033 ± 0.1
Size at first brood (F)	0 ± 0	0 ± 0	0.01 ± 0	0.01 ± 0	0 ± 0.2	0.097 ± 0.11
First brood size (F)	0.78 ± 1.96	0.12 ± 2.14	8.86 ± 1.09	9.76 ± 0.89	0.08 ± 0.2	0.092 ± 0.1
Interbrood period (F)	0 ± 0	0 ± 0	0.01 ± 0	0.02 ± 0	0.17 ± 0.27	0.302 ± 0.12
First brood offspring weight (F)	0 ± 0.02	0.03 ± 0.03	0.06 ± 0.01	0.09 ± 0.01	0 ± 0.28	0.334 ± 0.12
Age at maturity (M)	0 ± 0	0.004 ± 0	0.009 ± 0	0.013 ± 0	0 ± 0.2	0.313 ± 0.09
Size at maturity (M)	0 ± 0.07	0.156 ± 0.08	0.203 ± 0.03	0.358 ± 0.03	0 ± 0.18	0.434 ± 0.09

We repeated the analysis on each chromosome to test whether these estimates could be explained disproportionately by certain chromosomes, or whether per-chromosome associations may exist that cannot be observed within genome-wide estimates. Estimates of h^2c based on single chromosome GRMs revealed six chromosomes significantly associated with male size at maturity, four chromosomes with male age at maturity, and one chromosome with offspring weight (FDR ≤ 0.05; Table S7; Figure 2A). Of these however, according to the LRT approach only three chromosomes for male size at maturity (chr5: 20.7%, chr23: 13.9%, chr11: 13.3%), two for male age at maturity (chr1: 14.7%, chr10: 14.4%) and one for offspring weight (chr19: 8.4%) were significantly associated (LRT $p \leq$ 0.05; Table S5). Following multiple-testing correction within phenotypes, only the associations between chr5 and male size at maturity (LRT = 9.346, *fdr* = 0.046), and chr19 and offspring weight (LRT = 9.264, *fdr* = 0.046) were significantly associated according to both methods. Agreement between both methods was good according to a correlation of p-values (Spearman's ρ = 0.827, $p <$ 2.2e-16). Whilst the correlation here is strong, there is a clear downward biasing of p-values from single chromosome GRMs, evident as a shift away from the y=x relationship (Figure S3).

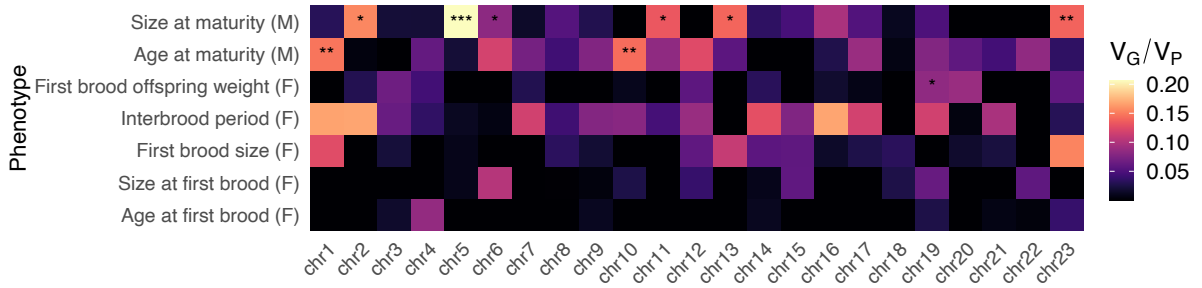

Figure 2: Estimates of phenotypic variance proportions explained by per-chromosome genetic relatedness matrices (h^2c). Tiles are coloured according to the relative proportion of genetic variance (V_G) to phenotypic variance (V_P). FDR-corrected p-values (corrected within phenotypes across all chromosomes) are displayed as asterisks FDR ≤ 0.05 = *; FDR ≤ 0.01 = **; FDR ≤ 0.001 = ***).

We found positive correlations associated with single chromosome GRM estimates of h^2c and chromosome size (following the addition of scaffold sizes according to the linkage map; Figure S4) for interbrood period (r = 0.373, p = 0.04, HC-corrected p = 0.105) and male size at maturity (r = 0.253, p = 0.122, HC-corrected p = 231), however these were not significant following HC-correction.

QTL mapping

We first mapped sex as a binary trait. The location of the sex-determining locus has been narrowed down to a small region at the distal end of chromosome 12 (Fraser *et al.*, 2020; Charlesworth, Bergero, *et al.*, 2020). Our QTL mapping recovered a single large peak on chromosome 12 (17.79 cM), with confidence intervals extending from 5.35-27.78 cM (Figure S5). In our map, the region following this (27.78-61.79 cM) corresponds to the very distal tip of chromosome 12 (approximately 24.6 Mb onwards, plus additionally placed scaffolds), which is the only fully recombining region of this chromosome and is pseudoautosomal (Charlesworth, Zhang, *et al.*, 2020). This places the sex-determining region somewhere in

the non-recombining region immediately prior to the pseudoautosomal region (PAR), as proposed by others (Fraser *et al.*, 2020; Charlesworth, Bergero, *et al.*, 2020). This analysis therefore confirms good power to detect loci of large effect and confirms previously published information about the sex chromosome and region containing the sex-determining locus.

We then mapped female traits using all fully informative markers (N = 1220) across all 267 females. Applying a permuted 5% threshold (N=1000), we detected two QTL. The strongest QTL was associated with first brood offspring weight at the very distal tip of chr19 (chr19:66.954) (Figure 3B), explained 7.46% of phenotypic variance, and exhibited additive effects in which the HH homozygotes produced smaller offspring than LL homozygotes (Figure 3C). Confidence intervals (drop in LOD of 1.5) extended between 55.335-67.877 cM. The other QTL was associated with size at first brood (chr22:63.593) (Figure 3D), explained 5.94% of phenotypic variance, and exhibited additive effects in which the HH homozygotes had their first brood at a larger size than LL homozygotes (Figure 3E); contrary to HP-LP expectations. Confidence intervals for the chromosome 22 QTL extended between 44.235 cM - 68.753 cM.

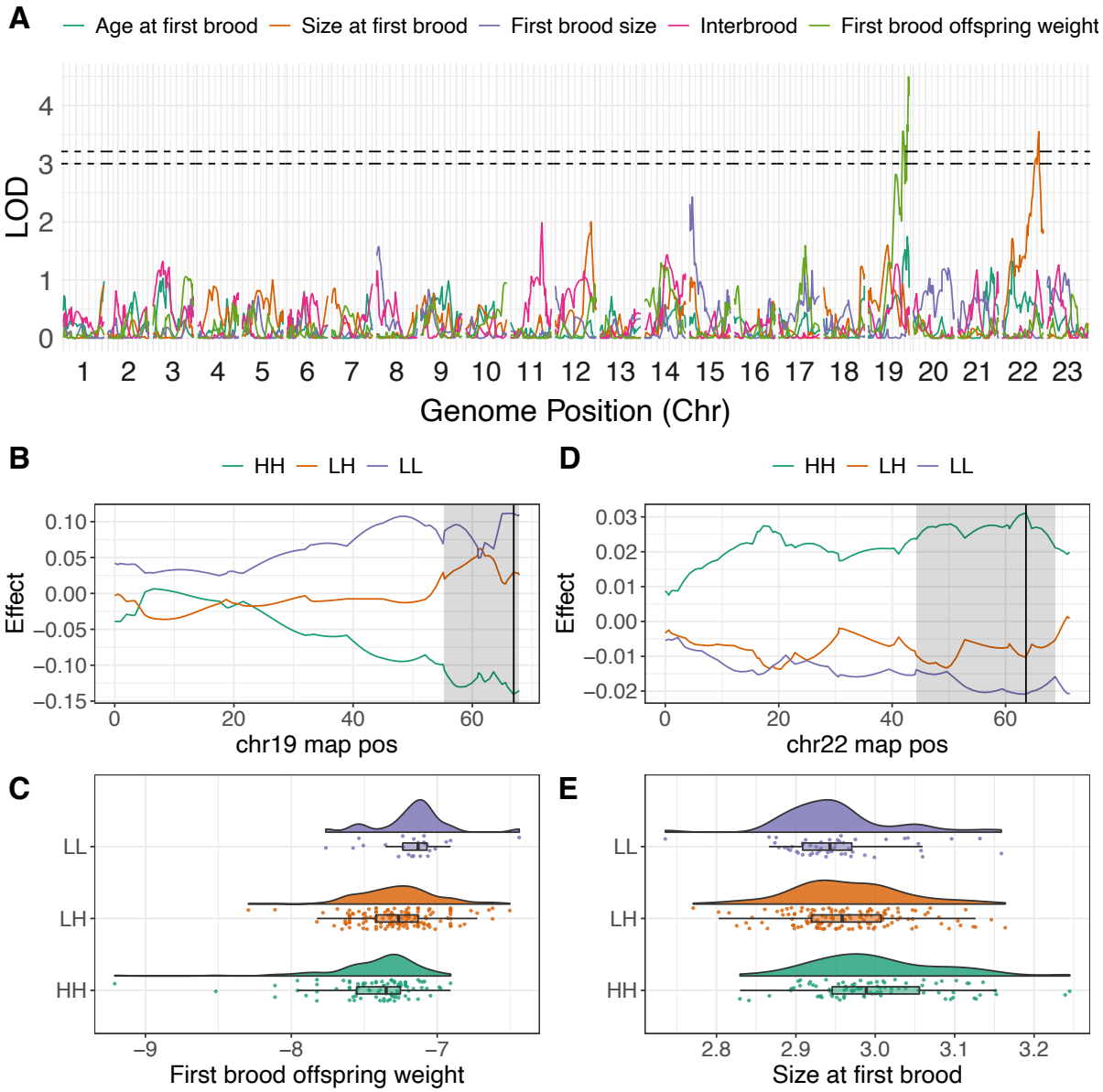

Figure 3: Single locus QTL scans for female life history traits: Age at first brood (days), size at first brood (cm), first brood size (residual), interbrood period (days) and first brood offspring weight (g). All female traits were log-transformed. Panel **A** shows genome-wide additive model scan results for all traits. 5% significance thresholds are denoted. Significant QTLs for offspring weight (chr19, **B**-**C**) and size at first brood (**D**-**E**) are visualised in further detail. Panels **B**-**E** show QTL effects across the focal linkage groups (**B** and **D**), and distributions of phenotypes across genotypes at the peak (**C** and **E**). In panels **B** and **D**, the QTL peak is shown as a black line, with confidence intervals (LOD drop = 1.5) highlighted by grey shaded areas.

Scans within each of the four families identified an additional three QTL (Figure S6-7). Two of these were observed in cross YHF5QM6, associated with first brood size (chr23:37.33,

LOD = 3.386, ci low = 4.589 cM, ci high = 53.588 cM) and interbrood period (chr12:60.713, LOD = 3.406, ci low = 54.701 cM, ci high = 72.487 cM). These QTL explained 18.55% and 18.65% of phenotypic variance within their families respectively. The QTL linked with interbrood period here is particularly interesting given its proximity to the sex-determining region. We also detected a QTL associated with female interbrood period in cross QF4YHM8 (chr14:28.41, LOD = 3.559, ci low = 28.412 cM, ci high = 67.316 cM), explaining 17.9% of phenotypic variance for this trait in this family.

We applied the same methodology to male traits, however we did not recover any significant QTLs across the whole dataset (Figure 4). Within the YHF6QM7 cross, we observed a significant QTL associated with male mature length on chromosome 23 (chr23:31.741, LOD = 3.462, ci low = 0 cM, ci high = 52.193 cM) (Figure S8-9). This confidence interval covered the majority of the chromosome, and the QTL explained 9.48% of phenotypic variance in this cross. At this QTL, HP homozygotes matured at a smaller size than LP homozygotes.

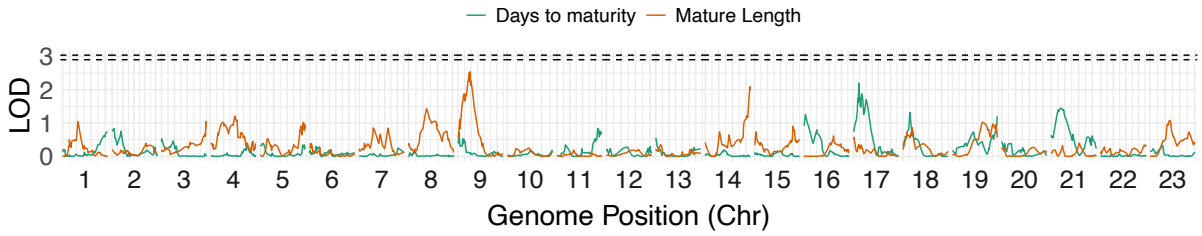

Figure 4: Single locus QTL scans for male life history traits: Days to maturity (log-transformed), length at maturity (mm). No significant QTLs were detected.

We also explored multi-QTL models using r/qtl's *stepwiseqtl()*, allowing for models that fit up to six loci, with the same additive covariance matrices of family and rearing covariates

used previously. For female models, this approach returned null models for all phenotypes except size at first brood and offspring weight, for which we recovered single QTL models including only the QTL loci previously identified above. For males, null models were returned for both phenotypes.

Candidate genes

Taken together, we find that where traits are heritable, they are associated with whole chromosomes, suggestive of large polygenic regions, rather than single large effect QTL. However, we observed two significant QTL for female traits (offspring weight chr19:66.954 and size at first brood chr22:63.593). We also observe several significant QTL within specific families. Of these, the QTL associated with interbrood in cross YHF5QM6 (YHF5QM6-chr12:60.71) is of particular interest given its proximity to the sex-determining region and relatively narrow confidence intervals. We therefore explored these three regions further for candidate genes. Full information on candidate genes can be found in Table S8.

The QTL at chr19:66.954, associated with offspring weight, covered ~8.2 Mb of chromosome 19, and included 267 genes. Due to the large size of this region, and that alternative confidence intervals (Bayesian 5% probability intervals) suggested a single peak at chr19:66.954, we limited our curation of candidate genes to the immediate 0.5 Mb either side of the peak (chr19:18602889-19602889). This region included 40 genes. Several of these genes (*wfikkn2b*, *tob1b*, *sap30bp*, *h3-3b*, *unk*, *mrpl38*, *fdxr*, *narf*, *cybc1*) are expressed in all stages of embryonic development in zebrafish, or interact with growth signalling pathways, suggesting potential functional effects for offspring weight. The closest gene to the peak was *cdr2l*. Of the 40 genes in this region, 18 exhibited female-biased differential

490 expression in gonads based on the guppy transcriptome (Sharma *et al.*, 2014), and six
491 exhibited male-biased expression (Table S8), suggesting potential reproductive function.
492
493 The chr22 QTL peak (for size at first brood) was on a previously unplaced scaffold
494 000111F_0:651336 and confidence intervals extended over the scaffold (00111F_0:528180-
495 1199617) and a region at the distal end of chromosome 22 (chr22:23415429-24223839).
496 The peak of the QTL did not overlap any genes, however the closest gene was F-box protein
497 33, *fbxo33*. In total, the region included 45 genes. There were no genes with GO terms or
498 KEGG annotations indicative of clear roles in growth. According to the GeneCards database
499 however, several genes had evidence of affecting size and growth phenotypes in mice
500 knockout studies (*fbxo33*, *tonsl*, *cnr1*, *cga*, *htr1b* and *myo6*). Two of the genes (*cga* and
501 *htr1b*) in this region are also associated with various hormonal pathways, including
502 gonadotropin hormone signalling that may affect development. Other genes in this region
503 are associated with myogenesis, including *myo6* and genes within the Akirin family (*akirin2*,
504 *gabrr1*, *pm20d2*, *cnr1*, *syncripl*). In addition, the gene *snx14* has been associated with
505 growth QTLs in grass carp (Huang *et al.*, 2020).
506
507 The interbrood period QTL on chr12 overlapped the YTH domain containing 1 gene, *ythdc1*,
508 on a previously unplaced scaffold 000149F_0 (000149F_0: 131600). This scaffold was placed
509 at the distal end of chromosome 12 near the sex-determining region, and corresponds with
510 scaffold KK215301.1 in the older female genome (Künstner *et al.*, 2016), which has similarly
511 been placed at the distal end of chromosome 12 in other mapping studies (Charlesworth,
512 Bergero, *et al.*, 2020). The confidence interval around this QTL covered additional regions of
513 scaffold 000149F_0 (000149F_0:47124-197258) and chromosome 12 (chr12:24525856-

24705290). This region included 18 genes, but none were associated with clear GO or KEGG terms indicative of roles for female fertility. Four genes exhibited female-biased expression in gonads and seven were male-biased. The gene overlapping the QTL peak, *ythdc1*, however is a promising candidate due to its interactions with N6-methyladenosine (m^6A) (Wang *et al.*, 2015; Xia *et al.*, 2018). Disruption of m^6A by mutation of another modifier *mettl3*, affected oocyte development and reduced the proportion of full-growth follicles in zebrafish (Xia *et al.*, 2018). Further, *Ythdc1*-deficient mice have oocyte maturation blocked at the primary follicle stage and experience alternative splicing defects in oocytes (Kasowitz *et al.*, 2018). Examination of transcripts matching *ythdc1* (largest = CUFF_24477_m.316355) in the guppy transcriptome (2014) revealed significant overexpression in ovaries compared with testes. Sequence analysis alongside other Poeciliids (Ensembl release 101: *P. formosa, P. latipinna, P. mexicana,* and *Xiphophorus maculeatus*) demonstrated significant purifying selection on this gene ($dN/dS \leq 0.197$; Z-tests for purifying selection: $2.79 \leq Z \leq 7.40$; Table S9). These provide strong evidence for a functional reproductive role for this gene in guppies.

DISCUSSION

Using an F2 cross design of outbred populations with divergent life history phenotypes, we have demonstrated both polygenic and oligogenic trait architectures underlying guppy life history evolution. For both male size and age at maturity, we find significant heritability associated with particular chromosomes, suggesting polygenic traits, but little evidence of a genome-wide signal of polygenicity or single loci of large effects. For the five females traits, we recovered significant genome-wide estimates of heritability associated with interbrood period and offspring weight. For offspring weight, all per-chromosome estimates of

538 heritability were generally weak, but we did identify a single locus of large effect at the
539 distal end of chromosome 19, suggesting an oligogenic architecture. For interbrood period,
540 we detected a weak genome-wide polygenic signal as an association between chromosome
541 size and per-chromosome heritability and also found evidence of a single locus of large
542 effect on the sex chromosome, LG12, in a single family. Together, these results suggest
543 interbrood period has an oligogenic genetic architecture consisting of a combination of
544 genome-wide polygenic loci and an individual locus of larger effect. We also detected a
545 significant single-locus QTL associated with female size at first brood with a small effect size,
546 but negligible estimates of genome-wide heritability for this trait. Finally, we found no
547 evidence for heritable genetic architectures for female first brood size and age at first
548 brood, although we observed a within-family QTL associated with first brood size on chr23.
549
550 The significant genetic components of guppy life history phenotypes found here are in line
551 with previous laboratory rearing estimates of heritability; specifically, the high heritability of
552 male traits, interbrood period, and offspring weight has been documented in laboratory-
553 reared populations under controlled conditions (Reznick, 1982) and in LP-introduction
554 experiments (Reznick *et al.*, 1997). However, there is mixed support for the heritability of
555 female life history traits. Consistent differences between laboratory-reared HP and LP
556 populations for female size and age at maturity and interbrood period have been observed
557 (Reznick, 1982), and similarly, Torres-Dowdall et al. (2012) report consistent differences in
558 female life history traits along a predation gradient in wild-caught vs lab-reared guppies
559 from the Guanapo river. However, estimates of heritability of female age and size at
560 maturity from experimental LP-introductions have shown inconsistent, often negligible,
561 estimates of heritability (Reznick *et al.*, 1997). Interestingly, this latter study postulates that

562 the higher heritability, and more rapid evolution, of male life history traits may involve
563 significant loci associated with the Y chromosome, but we found no evidence here to
564 support this (although see discussion about Y-linked male traits below). Rather, our results
565 of a significant polygenic component of male age and size at maturity also predicts more
566 rapid phenotypic evolution for males, as observed in experimental introductions (Reznick *et*
567 *al.*, 1997).
568
569 Recent work has sought to compare the relative contributions of genetic and plastic effects
570 on guppy life history. HP-LP comparisons are confounded by increased competition for
571 available resources at high densities in LP sites (Reznick *et al.*, 2001), which can result in life
572 history traits that are resource dependent. Across multiple laboratory-reared guppy crosses,
573 Felmy et al. (2021), demonstrated that guppy life histories cluster together in terms of those
574 strongly affected by resource plasticity (predominantly size-related traits), those affected by
575 HP-LP ecotype (including interbrood interval and offspring weight), and those affected by
576 both or neither. For female traits, these results align well with ours, particularly the higher
577 within-family heritability for interbrood period and offspring weight (Table 1), and the
578 absence of strong signatures of genetic architectures associated with female size at
579 maturity. The phenotypic covariances for female traits observed here (Table S6) also agree
580 with the proposed "mosaic" of guppy life history traits (Felmy *et al.*, 2021). Felmy et al.
581 (2021) also demonstrate resource-based plasticity for male age and size at maturity,
582 however these likely operate alongside underlying genetics, in agreement with observations
583 here, and documented in other studies of male guppy life history (Reznick, 1982; Reznick *et*
584 *al.*, 1997, 2005).
585

586 Guppy life history traits are also plastic with respect to other features of local environments.
587 Predator cues, for example, influence female size at maturity (Torres-Dowdall *et al.*, 2012)
588 and growth rate (Handelsman *et al.*, 2013), and resource availability affects female
589 reproductive investment (Reznick and Yang, 1993), the latter contributing comparable
590 phenotypic variance to that associated with heritability. We also found significant
591 associations between rearing conditions for both male age and size at maturity and female
592 age at first brood and interbrood period. These rearing effects reflected small fluctuations in
593 temperature (rearing temperature varied between 23.3-27.1 °C) and date of birth (used as a
594 proxy for other unmeasured rearing conditions), suggesting additional plasticity associated
595 with these phenotypes. Whilst we included rearing effects and family classification as
596 covariates in our models, and controlled for resources during rearing, it is quite possible
597 that additional sources of phenotypic plasticity may have obscured our analyses.
598
599 A limitation of our crossing design is that we cannot make across-family comparisons. We
600 controlled for family-specific intercepts in models, either by including kinship information or
601 family status as covariates. However, family status accounted for significant phenotypic
602 variance in five of our seven phenotypes (all except interbrood period and female age at
603 first brood; Table S4). These may be attributed to family-specific alleles segregating across
604 the genome, or Y-specifically, however we cannot separate these within the current dataset.
605 We identified some large effect loci segregating within families (Figure S6-9), however our
606 mapping of male phenotypes in particular will be blind to Y-specific QTL, given all males
607 within a family share the same Y allele. Y-linked loci have been suggested to affect age and
608 size at maturity phenotypes in other poeciliids (Kallman and Borkoski, 1978; Lampert *et al.*,

609 2010), so there is reason to assume these regions may be important and comprise some of
610 the phenotypic variance associated with family status (which is an upper limit).
611
612 Whilst we detected both polygenic and single-locus architectures for life history
613 phenotypes, our study is limited by sample size. In part this is due to the modest brood sizes
614 of guppies, which restricted our ability to generate larger F2 families, and also because the
615 phenotypes considered are sex-specific. It is well known within quantitative genetics studies
616 that small sample sizes can inflate estimates of heritability and QTL effect sizes, a
617 phenomenon termed the "Beavis Effect" (Beavis, 1994; Rockman, 2012; Slate, 2013). In
618 particular, sample size has been demonstrated to inflate p-values when run with single
619 chromosome GRMs with GCTA (Kemppainen and Husby, 2018a), which explains why we
620 recover more modest p-values when comparing single chromosome GRM results to the LRT
621 approach. Our estimates of per-chromosome (h^2c) and genome-wide heritability should
622 therefore be treated with caution. More generally, this combined approach of using single
623 chromosome GRMs and LRTs may be a useful strategy to alleviate issues with modest
624 sample sizes associated with each approach individually. Specifically, this refers to the
625 inflation of significance tests with single chromosome GRMs and issues with model
626 convergence for chromosomes with minimal effects under the LRT approach.
627
628 The two main QTL observed here, detected across the whole dataset, reflect only marginal
629 PVE (7.46% for offspring weight on chr19, and 5.94% for female size at first brood on chr22)
630 which is likely inflated by our low sample size. Interestingly, each of these chromosome-
631 phenotype pairings was also detected (marginal significance) by our multi-locus approaches.
632 This suggests that these regions may be reasonably large, such that the peak (from which

633 the PVE is calculated) only represents a portion of the variance explained by the wider
634 region. Neither of these regions have been strongly implicated in HP-LP adaptation before in
635 previous population genomic analyses (Fraser *et al.*, 2015; Whiting *et al.*, 2020), however
636 Whiting et al. (2020) recorded a selection scan outlier within the chr22 QTL interval
637 (chr22:23960000-23970000) in HP-LP comparisons from the Aripo and Madamas rivers. The
638 closest gene to this outlier is *sox11a*. While selection scans of HP-LP comparisons are unable
639 to determine which phenotype selection might be acting on, our results here suggest this
640 region may be involved in female growth.
641
642 An absence of prominent large effect loci, as described here for the majority of the traits,
643 would be expected to produce minimal molecular convergent evolution. This is predicted
644 due to redundancy in the mapping of genotype to phenotype, which may allow replicate
645 HP-LP pairs to use different sets of alleles to produce convergent HP-LP phenotypes (Barghi
646 *et al.*, 2020). Limited genomic convergence has been observed in two independent
647 evaluations of natural HP-LP populations (Fraser *et al.*, 2015; Whiting *et al.*, 2020), but
648 appears to be more pervasive in experimental translocations of HP guppies to previously
649 uncolonised LP habitats than naturally colonised LP populations (Fraser *et al.*, 2015). Part of
650 this discrepancy can be explained by the concept of “adaptive architecture”, such that the
651 convergent genetic basis of polygenic traits can be influenced by additional factors such as
652 starting allele frequencies. Starting allele frequencies or amounts of standing variation are
653 likely to be more similar when experimental populations are founded from the same
654 population and/or lack founding bottlenecks compared with naturally-derived HP-LP pairs in
655 different rivers. Empirical evidence for genetic convergence occurring with polygenic traits
656 has been observed for male mating song traits in Hawaiian *Laupala* crickets (Blankers *et al.*,

2019) and myxomatosis resistance in rabbits (Alves *et al.*, 2019), suggesting that genetic architecture alone is not necessarily a constraint on genetic convergence.

Similarly, polygenic traits are predicted to facilitate rapid adaptation. Several experimental studies involving the translocation of guppies into upstream LP habitats (Reznick and Bryga, 1987; Reznick *et al.*, 1997, 2019; Gordon *et al.*, 2009) or manipulating predation within populations (Reznick *et al.*, 1990) have demonstrated that HP-LP adaptive traits evolve rapidly over the course of a few generations. Our findings here, that some of these traits exhibit genetic architectures of many loci of small effect, are in keeping with recent empirical (Barghi *et al.*, 2019) and theoretical work (Bell, 2013; Jain and Stephan, 2017a) suggesting these facilitate rapid adaptation. In this framework, many loci of small effect provide adaptive substrate within populations to rapidly respond to shifting optima. This is particularly true if distance to new fitness optima is short, such that environmental change is modest and fitness effects are relative and/or non-lethal. This may be the case for guppy life history traits under LP regimes, where soft selection is most likely. This model therefore could allow male life history traits to change rapidly through small changes at many loci, whilst additional segregating larger effect loci may act in concert with compensatory changes at small effect loci for female traits. Our results here provide regions of the genome and candidate genes to explore further. For instance, an appreciation that much of the genetic basis of guppy life history traits may be polygenic informs on experimental and sampling designs for future population genetic studies of this system. In particular, temporal sampling and quantifying genome-wide autocovariances of neutral allele frequencies offers a promising avenue for studying the role of polygenic architectures in rapid adaptation

(Buffalo and Coop, 2019). The genomic regions identified here may serve as focal regions in these studies.

In conclusion, we used an F2 cross to explore the genetic architecture of seven guppy life history traits that are known to evolve rapidly and convergently in natural populations. We find evidence of only two loci of large effect associated with female size at first brood and offspring weight, and evidence of many loci of small effect associated with male age and size at maturity, interbrood period and brood size. In addition, we observed several within-family loci of large effect, suggesting segregating variation within source populations. These results have important implications for improving our understanding of how life history traits evolve in the guppy model, and more broadly, provide empirical evidence for predictions of the genetic architecture of rapidly adapting and convergent phenotypes.

ACKNOWLEDGEMENTS

The authors wish to thank all members of the Fraser group for useful discussions. Pasi Rastas provided advice for linkage mapping with Lep-MAP3. Simon Zhu, Blanca Guzman, Sara Ruckman, Ruchittrani Hapuarachchi, Christopher Tan, Kevin Khuu, Vicent Poon, Carol Villacana, and Brianna Paramo assisted in fish rearing and crossing at UC Riverside. HPC infrastructure support was provided by The University of Exeter's High Performance Computing (HPC) facility (ISCA). DNA sequencing was performed by University of Exeter Sequencing Service (ESS).

FUNDING

JRW, PJP, and BAF are supported by an EU Research Council Grant (GuppyCON 758382), JRP is supported by a NERC grant (NE/P013074/1). This project utilised equipment funded by the Wellcome Trust Institutional Strategic Support Fund (WT097835MF), Wellcome Trust Multi User Equipment Award (WT101650MA) and BBSRC LOLA award (BB/K003240/1).

DATA AVAILABILITY

All sequencing read data is available from the ENA (DOI: XXX)

All scripts and other data associated with analysis will be made available in an archived github repository (Zenodo, DOI: XXX)

CONFLICTS OF INTEREST

The authors declare no conflicts of interest.

REFERENCES

Alves JM, Carneiro M, Cheng JY, Lemos de Matos A, Rahman MM, Loog L, *et al.* (2019). Parallel adaptation of rabbit populations to myxoma virus. *Science* **363**: 1319–1326.

Ayllon F, Kjærner-Semb E, Furmanek T, Wennevik V, Solberg MF, Dahle G, *et al.* (2015). The vgll3 Locus Controls Age at Maturity in Wild and Domesticated Atlantic Salmon (Salmo salar L.) Males. *PLoS Genet* **11**: e1005628.

Baird NA, Etter PD, Atwood TS, Currey MC, Shiver AL, Lewis ZA, *et al.* (2008). Rapid SNP discovery and genetic mapping using sequenced RAD markers. *PLoS One* **3**: e3376.

Barghi N, Hermisson J, Schlötterer C (2020). Polygenic adaptation: a unifying framework to understand positive selection. *Nat Rev Genet*.

Barghi N, Tobler R, Nolte V, Jakšić AM, Mallard F, Otte KA, *et al.* (2019). Genetic redundancy fuels polygenic adaptation in Drosophila. *PLoS Biol* **17**: e3000128.

Barson NJ, Aykanat T, Hindar K, Baranski M, Bolstad GH, Fiske P, *et al.* (2015). Sex-dependent dominance at a single locus maintains variation in age at maturity in salmon. *Nature* **528**: 405–408.

Barton NH, Etheridge AM, Véber A (2017). The infinitesimal model: Definition, derivation, and implications. *Theor Popul Biol* **118**: 50–73.

Beavis WD (1994). The power and deceit of QTL experiments: lessons from comparative QTL studies. In: *Proceedings of the forty-ninth annual corn and sorghum industry research conference*, Chicago, IL, pp 250–266.

Bell G (2013). Evolutionary rescue and the limits of adaptation. *Philos Trans R Soc Lond B Biol Sci* **368**: 20120080.

Bérénos C, Ellis PA, Pilkington JG, Lee SH, Gratten J, Pemberton JM (2015). Heterogeneity of genetic architecture of body size traits in a free-living population. *Mol Ecol* **24**: 1810–1830.

Bergero R, Gardner J, Bader B, Yong L, Charlesworth D (2019). Exaggerated heterochiasmy in a fish with sex-linked male coloration polymorphisms. *Proc Natl Acad Sci U S A* **116**: 6924–6931.

Blankers T, Oh KP, Shaw KL (2019). Parallel genomic architecture underlies repeated sexual signal divergence in Hawaiian Laupala crickets. *Proc Biol Sci* **286**: 20191479.

Broad Institute (2019). Picard Toolkit. *Broad Institute, GitHub repository*.

Broman KW, Gatti DM, Simecek P, Furlotte NA, Prins P, Sen Ś, *et al.* (2019). R/qtl2: Software for Mapping Quantitative Trait Loci with High-Dimensional Data and Multiparent Populations. *Genetics* **211**: 495–502.

Broman KW, Wu H, Sen Ś, Churchill GA (2003). R/qtl: QTL mapping in experimental crosses. *Bioinformatics* **19**: 889–890.

Buffalo V, Coop G (2019). The Linked Selection Signature of Rapid Adaptation in Temporal Genomic Data. *Genetics* **213**: 1007–1045.

Charlesworth D, Bergero R, Graham C, Gardner J, Yong L (2020). Locating the Sex Determining Region of Linkage Group 12 of Guppy (Poecilia reticulata). *G3* **10**: 3639–3649.

Charlesworth D, Zhang Y, Bergero R, Graham C, Gardner J, Yong L (2020). Using GC content to compare recombination patterns on the sex chromosomes and autosomes of the guppy, Poecilia reticulata, and its close outgroup species. *Mol Biol Evol*.

Colosimo PF (2005). Widespread Parallel Evolution in Sticklebacks by Repeated Fixation of Ectodysplasin Alleles. *Science* **307**: 1928–1933.

Dayan DI, Du X, Baris TZ, Wagner DN, Crawford DL, Oleksiak MF (2019). Population genomics of rapid evolution in natural populations: polygenic selection in response to power station thermal effluents. *BMC Evol Biol* **19**: 61.

Duntsch L, Tomotani BM, de Villemereuil P, Brekke P, Lee KD, Ewen JG, *et al.* (2020). Polygenic basis for adaptive morphological variation in a threatened Aotearoa | New Zealand bird, the hihi (Notiomystis cincta). *Proc Biol Sci* **287**: 20200948.

Endler JA (1980). Natural Selection on Color Patterns in Poecilia reticulata. *Evolution* **34**: 76–91.

Felmy A, Reznick DN, Travis J, Potter T, Coulson T (2021). Life histories as mosaics: plastic and genetic components differ among traits that underpin life-history strategies. *bioRxiv*: 2021.02.12.430905.

Fisher RA (1918). The correlation between relatives under the supposition of Mendelian inheritance. *Trans R Soc Edinb* **52**: 399–433.

771 Fisher RA (1930). *The genetical theory of natural selection*. Clarendon Press: Oxford, England.

772 Fraser BA, Künstner A, Reznick DN, Dreyer C, Weigel D (2015). Population genomics of natural and
773 experimental populations of guppies (Poecilia reticulata). *Mol Ecol* **24**: 389–408.

774 Fraser BA, Whiting JR, Paris JR, Weadick CJ, Parsons PJ, Charlesworth D, *et al.* (2020). Improved
775 reference genome uncovers novel sex-linked regions in the guppy (Poecilia reticulata). *Genome*
776 *Biol Evol*.

777 Gordon SP, Reznick DN, Kinnison MT, Bryant MJ, Weese DJ, Räsänen K, *et al.* (2009). Adaptive
778 Changes in Life History and Survival following a New Guppy Introduction. *Am Nat* **174**: 34–45.

779 Hall MC, Basten CJ, Willis JH (2006). Pleiotropic quantitative trait loci contribute to population
780 divergence in traits associated with life-history variation in Mimulus guttatus. *Genetics* **172**:
781 1829–1844.

782 Handelsman CA, Broder ED, Dalton CM, Ruell EW, Myrick CA, Reznick DN, *et al.* (2013). Predator-
783 induced phenotypic plasticity in metabolism and rate of growth: rapid adaptation to a novel
784 environment. *Integr Comp Biol* **53**: 975–988.

785 Hartig F (2020). DHARMa: Residual Diagnostics for Hierarchical (Multi-Level / Mixed) Regression
786 Models.

787 Huang X, Jiang Y, Zhang W, Cheng Y, Wang Y, Ma X, *et al.* (2020). Construction of a high-density
788 genetic map and mapping of growth related QTLs in the grass carp (Ctenopharyngodon idellus).
789 *BMC Genomics* **21**: 313.

790 Jain K, Stephan W (2015). Response of Polygenic Traits Under Stabilizing Selection and Mutation
791 When Loci Have Unequal Effects. *G3* **5**: 1065–1074.

792 Jain K, Stephan W (2017a). Rapid Adaptation of a Polygenic Trait After a Sudden Environmental Shift.
793 *Genetics* **206**: 389–406.

794 Jain K, Stephan W (2017b). Modes of Rapid Polygenic Adaptation. *Mol Biol Evol* **34**: 3169–3175.

795 Kallman KD, Borkoski V (1978). A Sex-Linked Gene Controlling the Onset of Sexual Maturity in
796 Female and Male Platyfish (XIPHOPHORUS MACULATUS), Fecundity in Females and Adult Size in
797 Males. *Genetics* **89**: 79–119.

798 Kasowitz SD, Ma J, Anderson SJ, Leu NA, Xu Y, Gregory BD, *et al.* (2018). Nuclear m6A reader YTHDC1
799 regulates alternative polyadenylation and splicing during mouse oocyte development. *PLoS*
800 *Genet* **14**: e1007412.

801 Kemppainen P, Husby A (2018a). Inference of genetic architecture from chromosome partitioning
802 analyses is sensitive to genome variation, sample size, heritability and effect size distribution.
803 *Mol Ecol Resour* **18**: 767–777.

804 Kemppainen P, Husby A (2018b). Accounting for heteroscedasticity and censoring in chromosome
805 partitioning analyses. *Evol Lett* **2**: 599–609.

806 Kodama M, Hard JJ, Naish KA (2018). Mapping of quantitative trait loci for temporal growth and age
807 at maturity in coho salmon: Evidence for genotype-by-sex interactions. *Mar Genomics* **38**: 33–
808 44.

Künstner A, Hoffmann M, Fraser BA, Kottler VA, Sharma E, Weigel D, *et al.* (2016). The Genome of the Trinidadian Guppy , Poecilia reticulata , and Variation in the Guanapo Population. *PLoS One*: 1–25.

Lampert KP, Schmidt C, Fischer P, Volff J-N, Hoffmann C, Muck J, *et al.* (2010). Determination of onset of sexual maturation and mating behavior by melanocortin receptor 4 polymorphisms. *Curr Biol* **20**: 1729–1734.

Láruson ÁJ, Yeaman S, Lotterhos KE (2020). The Importance of Genetic Redundancy in Evolution. *Trends Ecol Evol* **35**: 809–822.

Li H (2013). Aligning sequence reads, clone sequences and assembly contigs with BWA-MEM. *arXiv [q-bioGN]*.

Manolio TA, Collins FS, Cox NJ, Goldstein DB, Hindorff LA, Hunter DJ, *et al.* (2009). Finding the missing heritability of complex diseases. *Nature* **461**: 747–753.

Martin M (2011). Cutadapt removes adapter sequences from high-throughput sequencing reads. *EMBnet.journal* **17**: 10–12.

Miller MR, Dunham JP, Amores A, Cresko WA, Johnson EA (2007). Rapid and cost-effective polymorphism identification and genotyping using restriction site associated DNA (RAD) markers. *Genome Res* **17**: 240–248.

Moghadam HK, Poissant J, Fotherby H, Haidle L, Ferguson MM, Danzmann RG (2007). Quantitative trait loci for body weight, condition factor and age at sexual maturation in Arctic charr (Salvelinus alpinus): comparative analysis with rainbow trout (Oncorhynchus mykiss) and Atlantic salmon (Salmo salar). *Mol Genet Genomics* **277**: 647–661.

Nicholls JA, Double MC, Rowell DM, Magrath RD (2000). The Evolution of Cooperative and Pair Breeding in Thornbills Acanthiza (Pardalotidae). *J Avian Biol* **31**: 165–176.

Poland JA, Brown PJ, Sorrells ME, Jannink J-L (2012). Development of high-density genetic maps for barley and wheat using a novel two-enzyme genotyping-by-sequencing approach. *PLoS One* **7**: e32253.

Pritchard JK, Pickrell JK, Coop G (2010). The genetics of human adaptation: hard sweeps, soft sweeps, and polygenic adaptation. *Curr Biol* **20**: R208–15.

Rastas P (2017). Lep-MAP3: robust linkage mapping even for low-coverage whole genome sequencing data. *Bioinformatics* **33**: 3726–3732.

R Core Team (2020). R: A Language and Environment for Statistical Computing.

Reed RD, Papa R, Martin A, Hines HM, Counterman BA, Pardo-Diaz C, *et al.* (2011). optix drives the repeated convergent evolution of butterfly wing pattern mimicry. *Science* **333**: 1137–1141.

Reznick D (1982). The impact of predation on life history evolution in Trinidadian guppies: genetic basis of observed life history patterns. *Evolution* **36**: 1236–1250.

Reznick DN, Bassar RD, Handelsman CA, Ghalambor CK, Arendt J, Coulson T, *et al.* (2019). Eco-evolutionary feedbacks predict the time course of rapid life history evolution. *Am Nat* **194**: 705380.

Reznick D, Bryant M, Holmes D (2005). The Evolution of Senescence and Post-Reproductive Lifespan in Guppies (Poecilia reticulata). *PLoS Biol* **4**: e7.

Reznick DN, Bryant MJ, Roff D, Ghalambor CK, Ghalambor DE (2004). Effect of extrinsic mortality on the evolution of senescence in guppies. *Nature* **431**: 1095–1099.

Reznick DN, Bryga H (1987). Life-history evolution in guppies (Poecilia reticulata): 1. Phenotypic and genetic changes in an introduction experiment. *Evolution* **41**: 1370–1385.

Reznick DA, Bryga H, Endler JA (1990). Experimentally induced life-history evolution in a natural population. *Nature* **346**: 357–359.

Reznick D, Butler MJ Iv, Rodd H (2001). Life-history evolution in guppies. VII. The comparative ecology of high- and low-predation environments. *Am Nat* **157**: 126–140.

Reznick DN, Rodd FH, Cardenas M (1996). Life-History Evolution in Guppies (Poecilia reticulata: Poeciliidae). IV. Parallelism in Life-History Phenotypes. *Am Nat* **147**: 319–338.

Reznick DN, Shaw FH, Rodd FH, Shaw RG (1997). Evaluation of the Rate of Evolution in Natural Populations of Guppies. *Science* **275**: 1934–1937.

Reznick D, Yang AP (1993). The Influence of Fluctuating Resources on Life History: Patterns of Allocation and Plasticity in Female Guppies. *Ecology* **74**: 2011–2019.

Richardson DS, Jury FL, Blaakmeer K, Komdeur J, Burke T (2001). Parentage assignment and extra-group paternity in a cooperative breeder: the Seychelles warbler (Acrocephalus sechellensis). *Mol Ecol* **10**: 2263–2273.

Rochette NC, Rivera-Colón AG, Catchen JM (2019). Stacks 2: Analytical methods for paired-end sequencing improve RADseq-based population genomics. *Mol Ecol* **28**: 4737–4754.

Rockman MV (2012). The QTN program and the alleles that matter for evolution: all that's gold does not glitter. *Evolution* **66**: 1–17.

Santure AW, De Cauwer I, Robinson MR, Poissant J, Sheldon BC, Slate J (2013). Genomic dissection of variation in clutch size and egg mass in a wild great tit (Parus major) population. *Mol Ecol* **22**: 3949–3962.

Santure AW, Poissant J, De Cauwer I, van Oers K, Robinson MR, Quinn JL, *et al.* (2015). Replicated analysis of the genetic architecture of quantitative traits in two wild great tit populations. *Mol Ecol* **24**: 6148–6162.

Sharma E, Künstner A, Fraser BA, Zipprich G, Kottler VA, Henz SR, *et al.* (2014). Transcriptome assemblies for studying sex-biased gene expression in the guppy, Poecilia reticulata. *BMC Genomics* **15**: 400.

Slate J (2013). From beavis to beak color: a simulation study to examine how much qtl mapping can reveal about the genetic architecture of quantitative traits. *Evolution* **67**: 1251–1262.

Stanton-Geddes J, Yoder JB, Briskine R, Young ND, Tiffin P (2013). Estimating heritability using genomic data (J Hadfield, Ed.). *Methods Ecol Evol* **4**: 1151–1158.

Stern DL (2013). The genetic causes of convergent evolution. *Nat Rev Genet* **14**: 751–764.

Torres-Dowdall J, Handelsman CA, Reznick DN, Ghalambor CK (2012). Local adaptation and the

885 evolution of phenotypic plasticity in Trinidadian guppies (Poecilia reticulata). *Evolution* **66**:
886 3432–3443.

887 Torres Dowdall J, Handelsman CA, Ruell EW, Auer SK, Reznick DN, Ghalambor CK (2012). Fine-scale
888 local adaptation in life histories along a continuous environmental gradient in Trinidadian
889 guppies: Fine-scale local adaptation in guppies. *Funct Ecol* **26**: 616–627.

890 Wang X, Zhao BS, Roundtree IA, Lu Z, Han D, Ma H, *et al.* (2015). N(6)-methyladenosine Modulates
891 Messenger RNA Translation Efficiency. *Cell* **161**: 1388–1399.

892 Westram AM, Rafajlović M, Chaube P, Faria R, Larsson T, Panova M, *et al.* (2018). Clines on the
893 seashore: The genomic architecture underlying rapid divergence in the face of gene flow. *Evol*
894 *Lett* **2**: 297–309.

895 Whitehead A, Clark BW, Reid NM, Hahn ME, Nacci D (2017). When evolution is the solution to
896 pollution: Key principles, and lessons from rapid repeated adaptation of killifish (Fundulus
897 heteroclitus) populations. *Evol Appl* **10**: 762–783.

898 Whiting JR, Paris JR, van der Zee MJ, Parsons PJ, Weigel D, Fraser BA (2020). Drainage-structuring of
899 ancestral variation and a common functional pathway shape limited genomic convergence in
900 natural high- and low-predation guppies. *bioRxiv*: 2020.10.14.339333.

901 Xia H, Zhong C, Wu X, Chen J, Tao B, Xia X, *et al.* (2018). Mettl3 Mutation Disrupts Gamete
902 Maturation and Reduces Fertility in Zebrafish. *Genetics* **208**: 729–743.

903 Yang J, Benyamin B, McEvoy BP, Gordon S, Henders AK, Nyholt DR, *et al.* (2010). Common SNPs
904 explain a large proportion of the heritability for human height. *Nat Genet* **42**: 565–569.

905 Yang J, Lee SH, Goddard ME, Visscher PM (2011). GCTA: a tool for genome-wide complex trait
906 analysis. *Am J Hum Genet* **88**: 76–82.

907 Yang J, Manolio TA, Pasquale LR, Boerwinkle E, Caporaso N, Cunningham JM, *et al.* (2011). Genome
908 partitioning of genetic variation for complex traits using common SNPs. *Nat Genet* **43**: 519–525.

909 Yeaman S, Gerstein AC, Hodgins KA, Whitlock MC (2018). Quantifying how constraints limit the
910 diversity of viable routes to adaptation. *PLoS Genet* **14**: e1007717.

911 Zhang D (2020). rsq: R-Squared and Related Measures.

912